Proton-electron mass ratio from laser spectroscopy of HD+ at the part-per-trillion level

Patra, Sayan; Germann, M.; Karr, J. Ph; Haidar, M.; Hilico, L.; Korobov, V. I.; Cozijn, F. M.J.; Eikema, K. S.E.; Ubachs, W.; Koelemeij, J. C.J.

published in
Science (New York, N.Y.)
2020

DOI (link to publisher)
10.1126/science.aba0453

document version
Publisher's PDF, also known as Version of record

METROLOGY

Proton-electron mass ratio from laser spectroscopy of HD^+ at the part-per-trillion level

Sayan Patra[1], M. Germann[1]*, J.-Ph. Karr[2,3], M. Haidar[2], L. Hilico[2,3], V. I. Korobov[4], F. M. J. Cozijn[1], K. S. E. Eikema[1,5], W. Ubachs[1,5], J. C. J. Koelemeij[1]†

Recent mass measurements of light atomic nuclei in Penning traps have indicated possible inconsistencies in closely related physical constants such as the proton-electron and deuteron-proton mass ratios. These quantities also influence the predicted vibrational spectrum of the deuterated molecular hydrogen ion (HD^+) in its electronic ground state. We used Doppler-free two-photon laser spectroscopy to measure the frequency of the $v = 0 \rightarrow 9$ overtone transition (v, vibrational quantum number) of this spectrum with an uncertainty of 2.9 parts per trillion. By leveraging high-precision ab initio calculations, we converted our measurement to tight constraints on the proton-electron and deuteron-proton mass ratios, consistent with the most recent Penning trap determinations of these quantities. This results in a precision of 21 parts per trillion for the value of the proton-electron mass ratio.

Precision measurements on simple atomic systems and their constituents play an essential role in the determination of physical constants. Examples range from the proton-electron mass ratio (m_p/m_e), the value of which depends strongly on measurements performed on single protons and hydrogen-like ions stored in Penning traps, to the Rydberg constant (R_∞) and proton electric charge radius (r_p), which are derived from spectroscopic measurements of energy intervals in atomic hydrogen-like systems (*1*, *2*). It is desirable to perform such determinations of physical constants redundantly by using different systems and methods, as this provides a crucial cross-check for possible experimental inconsistencies or physical effects beyond our current understanding of nature. This need is illustrated by the proton radius puzzle, a 5.6σ discrepancy between the value of r_p obtained from muonic hydrogen spectroscopy and the 2014 Committee on Data for Science and Technology (CODATA-2014) reference value (*1*, *3*). Progress toward solution of the puzzle was made after most of the recent r_p determinations from electron-proton scattering and atomic hydrogen spectroscopy were found to be consistent with the muonic hydrogen value (*4*–*7*). A similar need for alternative measurements is indicated for m_p/m_e—an important dimensionless quantity that sets the scale of rotations and vibrations in molecules—because recent Penning trap measurements of the relative atomic masses of light atomic nuclei [including those of the proton (m_p), deuteron (m_d), and helion (m_h)] differed from earlier results by several standard deviations (*8*–*15*). For example, Heiße *et al.* (*11*) determined m_p with a precision of 32 parts per trillion (ppt), three times as high as the then-accepted CODATA-2014 value, but also found it to be smaller by 3σ (*11*, *12*). The value from (*11*) has been incorporated in the 2017 and 2018 CODATA adjustments, but uncertainty margins were increased by a factor of 1.7 to accommodate the difference (*2*). This uncertainty range currently limits the precision of m_p/m_e (obtained by dividing m_p by the more precise CODATA-2018 value of m_e) to 60 ppt, which in turn diminishes the predictive power of ab initio calculations of rotational-vibrational (rovibrational) spectra of molecular hydrogen ions (H_2^+ and HD^+) and antiprotonic helium, which have achieved a precision of 7 to 8 ppt (*16*).

The high theoretical precision, in principle, enables an improved determination of m_p/m_e from spectroscopy of molecular hydrogen ions, which could shed light on this situation (*17*). However, such an improvement requires measurements with uncertainties on the parts-per-trillion level, which is two orders of magnitude beyond that of state-of-the-art laser (*18*, *19*) and terahertz (*20*) spectroscopy of HD^+ and antiprotonic helium. Here, we present a frequency measurement of the (v,L): (0,3)→(9,3) vibrational transition (v, vibrational quantum number; L, rotational angular momentum quantum number) in the electronic ground state of HD^+ with 2.9-ppt uncertainty, which is notably more precise than the theoretical uncertainty. This finding allows us to extract a new value of m_p/m_e and provide a cross-link to other physical constants, which enables additional consistency checks of their values.

We previously identified the (v,L): (0,3)→(4,2)→(9,3) two-photon transition in HD^+ (Fig. 1A) as a promising candidate for high-resolution Doppler-free laser spectroscopy (*21*), owing to the near-degeneracy of the 1442- and 1445-nm photons, as well as the possibility of storing HD^+ ions in a linear Paul trap while cooling them to 10 mK through Coulomb interaction with cotrapped beryllium ions, which are themselves cooled by 313-nm laser radiation. We showed that for counterpropagating 1442- and 1445-nm laser beams directed along the trap's symmetry axis, Doppler-free vibrational excitation of HD^+ deep in the optical Lamb-Dicke regime may be achieved. Thus, with a natural linewidth of 13 Hz, quality factors of $>10^{13}$ become within reach. We used phase-stabilized, continuous-wave external cavity diode lasers at 1442 and 1445 nm with linewidths of 1 to 2 kHz to vibrationally excite cold, trapped HD^+ ions (*22*). Optical frequencies were measured with an uncertainty below 1 ppt using an optical frequency comb laser, whereas two-photon excitation was detected through enhanced loss of HD^+ from the trap, owing to state-selective dissociation of molecules in the $v = 9$ state by 532-nm laser radiation (*22*, *23*).

Rovibrational energy levels of HD^+ exhibit hyperfine structure caused by magnetic interactions between the spins of the proton ($\mathbf{I}_p$),

Table 1. Leading systematic shifts and uncertainties. Shifts and their standard uncertainties (in parentheses) are given in kilohertz. Their justification can be found in (*22*), as well as the complete error budget (table S2).

Description	$F = 0$ transition	$F = 1$ transition
dc Zeeman effect	0.02(1)	0.10(1)
ac Stark effect, 532-nm laser	0.41(10)	0.46(11)
ac Stark effect, 1442-nm laser	−0.06(1)	−0.01(0)
ac Stark effect, 1445-nm laser	0.03(1)	−0.11(3)
Optical frequency measurement	−0.02(42)	−0.02(42)
Total systematic shifts	**0.38(43)**	**0.42(43)**
Uncertainty of fitted optical transition frequencies	0.00(41)	0.00(51)
Total systematic shifts + fitted optical frequencies	**0.38(59)**	**0.42(66)**

[1]LaserLaB, Department of Physics and Astronomy, Vrije Universiteit Amsterdam, 1081 HV Amsterdam, Netherlands. [2]Laboratoire Kastler Brossel, UPMC–Sorbonne Université, CNRS, ENS-PSL Research University, Collège de France, 75005 Paris, France. [3]Département de Physique, Université d'Evry–Val d'Essonne, Université Paris-Saclay, 91000 Evry, France. [4]Bogolyubov Laboratory of Theoretical Physics, Joint Institute for Nuclear Research, Dubna 141980, Russia. [5]ARCNL (Advanced Research Centre for Nanolithography), 1098 XG Amsterdam, Netherlands.
*Present address: Department of Physics, Umeå University, 901 87 Umeå, Sweden.
†Corresponding author. Email: j.c.j.koelemeij@vu.nl

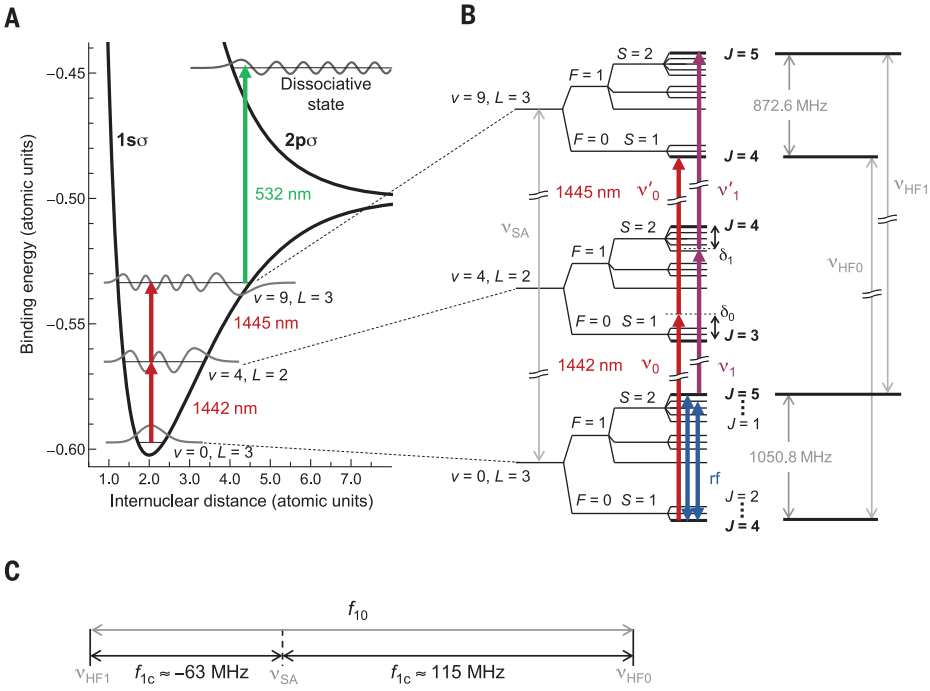

Fig. 1. Partial level diagram and multiphoton transitions. (**A**) Two-photon transitions are driven between rovibrational states with (v,L) = (0,3) and (9,3) in the 1sσ electronic ground state of HD^+. State-selective dissociation of the v = 9 population is induced through excitation to the antibonding 2pσ electronic state by a 532-nm photon. (**B**) Spin-averaged transition frequency (ν_{SA}) and hyperfine structure (not to scale) of the levels involved in the two-photon transition, as well as graphical definitions of the frequencies and detunings of the electromagnetic fields driving transitions between them. (**C**) Graphical definition of the hyperfine intervals in the two-photon transition.

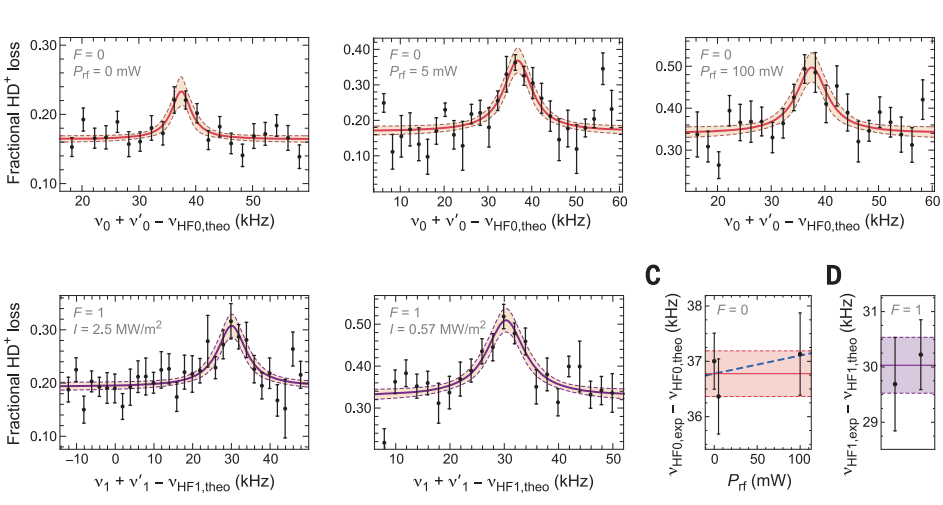

Fig. 2. Spectra of the two-photon transition at 415 THz. (**A**) Spectra of the F = 0 transition at various levels of the rf power (P_{rf}). Lorentzian line fits are shown along with 68% confidence level bands. Each data point represents the mean of a set of (typically) nine individual measurements, with error bars indicating SEM. (**B**) Spectral data and Lorentzian line fits for the F = 1 transitions at two different values of the 532-nm laser intensity (I). (**C**) Fitted line centers of the F = 0 transitions [corrected for systematic shifts (*22*)] shown in (A) are additionally used to check for a possible quasi-resonant ac Zeeman shift by fitting a linear model and extrapolating to P_{rf} = 0 mW. The fit (dashed blue line) implies no significant shift. The zero-field F = 0 frequency and uncertainty are indicated by the red horizontal line and pink bands, respectively. (**D**) F = 1 line-center frequencies from the fits shown in (B), after correction for systematic shifts (*22*). The purple line and bands indicate the weighted mean and uncertainty, respectively.

deuteron ($\mathbf{I}_d$), and electron ($\mathbf{s}_e$), as well as the molecule's rotational angular momentum ($\mathbf{L}$) (*24*). The spins are coupled to form resultant angular momenta $\mathbf{F} = \mathbf{s}_e + \mathbf{I}_p$ and $\mathbf{S} = \mathbf{F} + \mathbf{I}_d$ and are finally coupled with $\mathbf{L}$ to form the total angular momentum $\mathbf{J} = \mathbf{S} + \mathbf{L}$. We observed transitions (v,L; F,S,J): (0,3; 1,2,5)→(9,3; 1,2,5) (here referred to as the "F = 1 transition") and (v,L; F,S,J): (0,3; 0,1,4)→(9,3; 0,1,4) (the "F = 0 transition"); see Fig. 1B.

To record a spectrum, we kept the 1442-nm laser frequency (ν_F) (with F = 0,1; see Fig. 1B) at a fixed detuning (δ_F) from resonance to avoid excessive population of the intermediate v = 4 state (*21*, *22*). Meanwhile, we stepped the 1445-nm laser frequency (ν'_F) in intervals of 2 kHz over the range of interest (Fig. 1B). At each step, we let all lasers interact with the HD^+ ions for 30 s, after which we determined the cumulative loss of HD^+ and added the resulting data point to the spectrum (*22*). A typical spectrum covers a span of 40 to 60 kHz, with an average of nine points per frequency and with the 180 to 270 data points acquired in random order over ~10 measurement days. The signal-to-noise ratio of the F = 0 spectrum turned out to be lower than its F = 1 counterpart, which we attribute to a smaller available population in the initial state and slower repopulation by blackbody radiation (*21*). To increase the F = 0 signal, we applied two radio frequency (rf) magnetic fields to drive the population from the (F,S,J) = (1,2,5) and (1,2,4) states of the v = 0, L = 3 hyperfine manifold to the (F,S,J) = (0,1,4) states (see Fig. 1B and fig. S1) (*22*). Recorded spectra of the F = 0 and F = 1 transitions are shown in Fig. 2.

The interpretation of the recorded spectra requires analysis of several systematic effects that affect line shape and position (*22*). We exploit the good theoretical accessibility of the HD^+ molecule (*25*), which allows a priori estimation of these effects. Zeeman and Stark effects are calculated to shift the F = 0 and

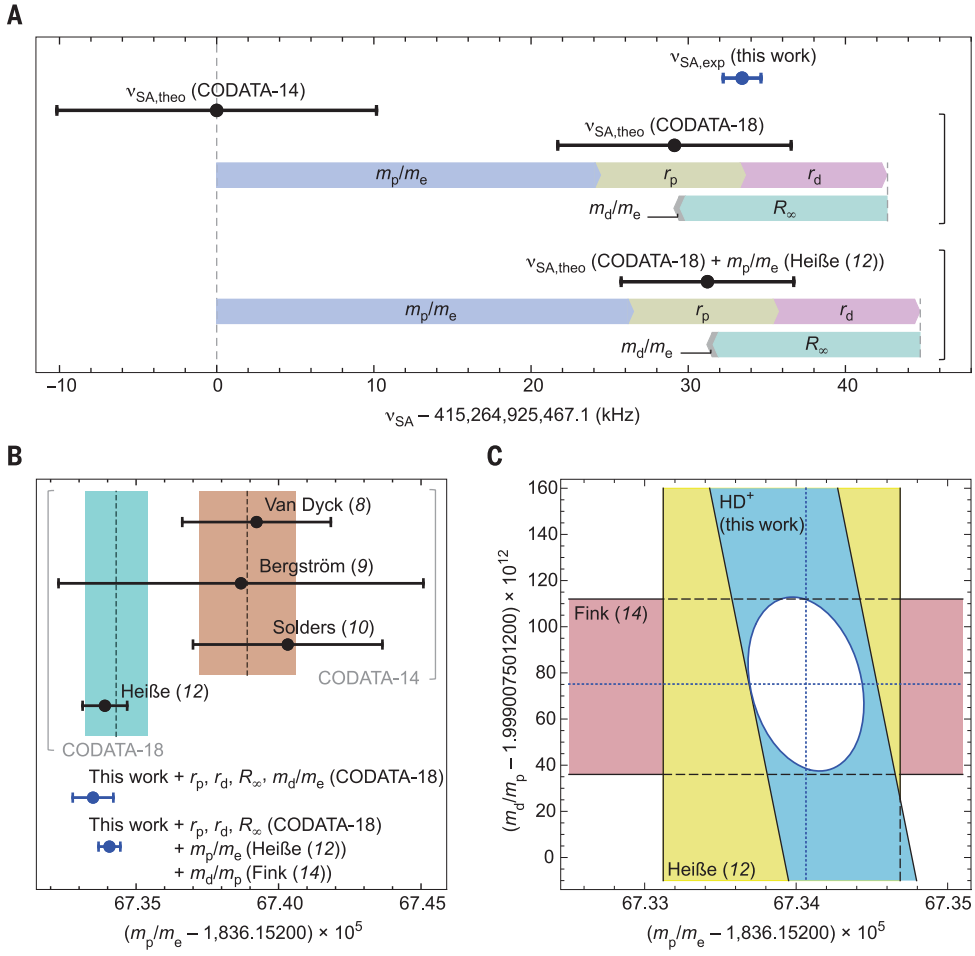

Fig. 3. Implications for the values of physical constants. (**A**) Comparison between $\nu_{SA,exp}$ and theoretical frequencies $\nu_{SA,theo}$ (k) obtained for the indicated combinations of physical constants, k. Arrows represent the cumulative frequency shift introduced by consecutively replacing the CODATA-2014 values of m_p/m_e (blue), r_p (yellow), r_d (purple), R_∞ (green), and m_d/m_e (gray) with their counterparts of the set k. Error bars indicate 1σ uncertainty. (**B**) Values and uncertainties of m_p/m_e from this work (blue data points) compared with measured m_p values from other sources, which were converted to values of m_p/m_e through division by m_e (CODATA-2018). The lowermost blue data point represents the value derived in (C). Dashed lines and shaded areas represent CODATA values and their ±1σ ranges, with brackets indicating which of the measurements shown were included in the respective CODATA adjustments. Error bars indicate 1σ uncertainty. (**C**) Simultaneous constraint on m_p/m_e and m_d/m_p from HD^+ and recent independent measurements of these quantities, leading to new values of m_p/m_e and m_d/m_p (blue dotted lines) and the corresponding 1σ-constrained region (white ellipse).

$F = 1$ lines by as much as 0.5 kHz through level shifting and line-shape deformation (*22*). The expected two-photon power broadening and interaction-time broadening from the 9×10^3 s^{-1} rate of dissociation of molecules in the $v = 9$ state (*21*) satisfactorily explain the observed linewidths of 8(3) kHz (number in parentheses denotes uncertainty). In addition, we experimentally investigated a number of systematic effects, yielding results consistent with the theory-based estimates (*22*). The sizes and uncertainties of leading systematic effects are listed in Table 1.

As shown in Fig. 2, Lorentzian line shapes are fitted to the spectra to determine their respective line centers with 0.6- to 0.7-kHz uncertainty. These are subsequently corrected for systematic frequency shifts and combined to arrive at the $F = 0$ and $F = 1$ transition frequencies: $\nu_{HF0,exp}$ and $\nu_{HF1,exp}$ (*22*) (see Fig. 2, C and D, and Table 2). These frequencies are related to the spin-averaged (i.e., pure rovibrational) frequency (ν_{SA}) through the relations $\nu_{SA} = \nu_{HF0} - f_{0c}$ and $\nu_{SA} = \nu_{HF1} - f_{1c}$ (f, hyperfine shift) (Fig. 1C). Because only ν_{SA} depends directly on the values of the physical constants of interest, we need to determine and correct for the hyperfine shifts $f_{1c} \approx -63$ MHz and $f_{0c} \approx 115$ MHz to derive ν_{SA}. We take the hyperfine intervals $f_{0c,theo}$ and $f_{1c,theo}$ from theory (*22*, *24*, *26*) and compute $\nu_{SA,exp}$ as the mean of $\nu_{HF0,exp} - f_{0c,theo}$ and $\nu_{HF1,exp} - f_{1c,theo}$ (*22*). In this process, we expand the uncertainties of the theoretical hyperfine intervals by about a factor of 2 (*22*) so that the theoretical hyperfine interval ($f_{10,theo}$)

Table 2. Experimental and theoretical transition frequencies and hyperfine intervals. Uncertainties are given in parentheses and justified in detail in (*22*). The uncertainties of hyperfine intervals include an expansion factor of ~2. During data acquisition and in Fig. 2, theoretical frequency values ($\nu_{HF0,theo}$ and $\nu_{HF1,theo}$) based on CODATA-2014 constants were used as offset values. All other theoretical frequency values were obtained from CODATA-2018 physical constants.

Symbol	Value (kHz)
$\nu_{HF0,theo}$*	415,265,040,466.8
$\nu_{HF1,theo}$*	415,264,862,219.1
$\nu_{HF0,exp}$	415,265,040,503.6(0.6)
$\nu_{HF1,exp}$	415,264,862,249.2(0.7)
$f_{0c,theo}$	114,999.7(1.9)
$f_{1c,theo}$	−63,248.0(2.1)
$f_{10,theo}$	178,247.7(3.3)
$f_{10,exp}$	178,254.4(0.9)
$\nu_{SA,theo}$	415,264,925,496.2(7.4)
$\nu_{SA,exp}$	415,264,925,500.5(1.2)

*Offset values based on CODATA-2014 constants (included for completeness).

becomes consistent with its measured counterpart ($f_{10,exp} \equiv \nu_{HF0,exp} - \nu_{HF1,exp}$) (Table 2). We thus find $\nu_{SA,exp}$ = 415,264,925,500.5(0.4)$_{exp}$ (1.1)$_{theo}$(1.2)$_{total}$ kHz.

Our experimental frequency $\nu_{SA,exp}$ exceeds the theoretical frequency $\nu_{SA,theo}$ (CODATA-2014) = 415,264,925,467.1(10.2) kHz by 33.4 kHz, or 3.3σ, when we use CODATA-2014 physical constants to compute $\nu_{SA,theo}$ (*22*, *27*). The uncertainties of these constants dominate the 10.2-kHz uncertainty rather than the 3.1-kHz precision of the theoretical model—e.g., m_p/m_e contributes 9.0 kHz (fig. S3) (*22*). Using known sensitivity coefficients (*17*, *22*), we can also compute other theoretical frequency values, $\nu_{SA,theo}$ (k), for other combinations (labeled k) of values of physical constants. For example, a more precise value is obtained by use of CODATA-2018 constants: $\nu_{SA,theo}$ (CODATA-2018) = 415,264,925,496.2(7.4) kHz. This state-of-the-art value is shifted by 29.1 kHz with respect to the CODATA-2014 value (Fig. 3A) and essentially closes the 33.4-kHz gap with our experimental value ($\nu_{SA,exp}$). Figure 3A furthermore shows that most of the 29.1-kHz shift stems from the smaller CODATA-2018 value of m_p/m_e. A smaller part, 5.1 kHz, is due to the CODATA-2018 updated values of r_p, r_d, and R_∞, which are essentially equal to the muonic hydrogen values (*3*, *28*). The 5.1-kHz shift, which is four times as large as our experimental uncertainty and comparable to the current theoretical precision, therefore reveals the impact of the proton radius puzzle on molecular vibrations. We obtain even better precision (5.5 kHz) and agreement after replacing the CODATA-2018 value of m_p/m_e with that from (*11*, *12*), this time leading to a 31.2-kHz shift (Fig. 3A).

We may also invert the procedure and derive a new value of m_p/m_e from the difference $\nu_{SA,exp} - \nu_{SA,theo}$ (k); see Fig. 3B. Using $\nu_{SA,theo}$ (CODATA-2018), we obtain m_p/m_e (HD^+) = 1,836.152673349(71), which is slightly more precise than, and in excellent agreement with, the value of m_p/m_e from (*12*). Because $\nu_{SA,theo}$ is also sensitive to the deuteron-proton mass ratio (*22*), one may alternatively extract a two-dimensional constraint in the (m_p/m_e, m_d/m_p) plane (Fig. 3C). Our result is in good agreement with both m_p/m_e from (*12*) and the recent value of m_d/m_p (*14*), assuming CODATA-2018 values of r_p, r_d, and R_∞. This justifies a determination of m_p/m_e from the combination of all three results shown in Fig. 3C, leading to a value of 1,836.152673406(38) (lowermost point in Fig. 3B) which, at 21-ppt precision, represents the most precise determination of this quantity to date. The data shown in Fig. 3C can furthermore be combined with the CODATA-2018 value of m_e and the value of m_h from (*15*) to obtain the atomic mass difference $m_p + m_d - m_h$ = 0.00589743254(12) u (where u is the unified atomic mass unit). The same quantity has previously been determined from the measured mass ratio $^3He^+/HD^+$ (*13*), leading to $m_p + m_d - m_h$ = 0.00589743219(7) u. The two results differ by 0.35(14) nu, or 2.5σ. We thereby confirm the "^{3}He puzzle," a term used to describe similar deviations of 0.48(10) nu (4.8σ) and 0.33(13) nu (2.4σ) reported earlier (*13*, *14*).

Our work establishes precision spectroscopy of HD^+, combined with ab initio quantum molecular calculations, as a state-of-the-art method for determining fundamental mass ratios. It furthermore provides a link between mass ratios and other physical constants, such as R_∞, and sheds light on the large deviations seen between recent determinations of their values. We anticipate that our results will have a notable impact on the consistency and precision of future reference values of physical constants and will enhance the predictive power of ab initio calculations of physical quantities.

Note added in proof: In a recent and independent study by Alighanbari *et al.* (*29*), a value for the proton-electron mass ratio comparable to ours was obtained from rotational spectroscopy of HD^+.

REFERENCES AND NOTES

1. P. J. Mohr, D. B. Newell, B. N. Taylor, *J. Phys. Chem. Ref. Data* **45**, 043102 (2016).
2. P. J. Mohr, D. B. Newell, B. N. Taylor, E. Tiesinga, *Metrologia* **55**, 125–146 (2018).
3. A. Antognini *et al.*, *Science* **339**, 417–420 (2013).
4. A. Beyer *et al.*, *Science* **358**, 79–85 (2017).
5. H. Fleurbaey *et al.*, *Phys. Rev. Lett.* **120**, 183001 (2018).
6. N. Bezginov *et al.*, *Science* **365**, 1007–1012 (2019).
7. W. Xiong *et al.*, *Nature* **575**, 147–150 (2019).
8. R. S. Van Dyck Jr., D. L. Farnham, S. L. Zafonte, P. B. Schwinberg, *AIP Conf. Proc.* **457**, 101–110 (1999).
9. I. Bergström, T. Fritioff, R. Schuch, J. Schönfelder, *Phys. Scr.* **66**, 201–207 (2002).
10. A. Solders, I. Bergström, S. Nagy, M. Suhonen, R. Schuch, *Phys. Rev. A* **78**, 012514 (2008).
11. F. Heiße *et al.*, *Phys. Rev. Lett.* **119**, 033001 (2017).
12. F. Heiße *et al.*, *Phys. Rev. A* **100**, 022518 (2019).
13. S. Hamzeloui, J. A. Smith, D. J. Fink, E. G. Myers, *Phys. Rev. A* **96**, 060501(R) (2017).
14. D. J. Fink, E. G. Myers, *Phys. Rev. Lett.* **124**, 013001 (2020).
15. S. L. Zafonte, R. S. Van Dyck Jr., *Metrologia* **52**, 280–290 (2015).
16. V. I. Korobov, L. Hilico, J.-Ph. Karr, *Phys. Rev. Lett.* **118**, 233001 (2017).
17. J.-Ph. Karr, L. Hilico, J. C. J. Koelemeij, V. I. Korobov, *Phys. Rev. A* **94**, 050501(R) (2016).
18. J. Biesheuvel *et al.*, *Nat. Commun.* **7**, 10385 (2016).
19. M. Hori *et al.*, *Science* **354**, 610–614 (2016).
20. S. Alighanbari, M. Hansen, V. I. Korobov, S. Schiller, *Nat. Phys.* **14**, 555–559 (2018).
21. V. Q. Tran, J.-Ph. Karr, A. Douillet, J. C. J. Koelemeij, L. Hilico, *Phys. Rev. A* **88**, 033421 (2013).
22. Materials and methods are available as supplementary materials.
23. J. Biesheuvel *et al.*, *Appl. Phys. B* **123**, 23 (2017).
24. D. Bakalov, V. I. Korobov, S. Schiller, *Phys. Rev. Lett.* **97**, 243001 (2006).
25. J.-Ph. Karr, *J. Mol. Spectrosc.* **300**, 37–43 (2014).
26. V. I. Korobov, J. C. J. Koelemeij, L. Hilico, J.-Ph. Karr, *Phys. Rev. Lett.* **116**, 053003 (2016).
27. D. T. Aznabayev, A. K. Bekbaev, V. I. Korobov, *Phys. Rev. A* **99**, 012501 (2019).
28. R. Pohl *et al.*, *Science* **353**, 669–673 (2016).
29. S. Alighanbari, G. S. Giri, F. L. Constantin, V. I. Korobov, S. Schiller, *Nature* **581**, 152–158 (2020).

ACKNOWLEDGMENTS

We thank R. Kortekaas, T. Pinkert, and the Electronic Engineering Group of the Faculty of Science at Vrije Universiteit Amsterdam for technical assistance. **Funding:** We acknowledge support from the Netherlands Organisation for Scientific Research (FOM Programs "Broken Mirrors & Drifting Constants" and "The Mysterious Size of the Proton"; FOM 13PR3109, STW Vidi 12346), the European Research Council (AdG 670168 Ubachs, AdG 695677 Eikema), the COST Action CA17113 TIPICQA, and the Dutch-French bilateral Van Gogh program. J.-Ph.K. acknowledges support as a fellow of the Institut Universitaire de France. V.I.K. acknowledges support from the Russian Foundation for Basic Research under grant ~19-02-00058-a. **Author contributions:** J.C.J.K. conceived the experiment; S.P., M.G., F.M.J.C., W.U., K.S.E.E., J.C.J.K., J.-Ph.K., and L.H. designed the experiment; J.-Ph.K., M.H., and V.I.K. developed the theory and performed numerical calculations; S.P., M.G., J.-Ph.K., M.H., L.H., and J.C.J.K. set up and performed numerical simulations for analysis of systematic effects; S.P., M.G., F.M.J.C., K.S.E.E., and J.C.J.K. built the experiment; S.P. and M.G. performed the measurements; S.P., M.G., and J.C.J.K. analyzed the data; S.P., M.G., and J.C.J.K. wrote the manuscript, with input from all other authors; and J.-Ph.K., L.H., K.S.E.E., W.U., and J.C.J.K. planned and supervised the project. **Competing interests:** One of the authors (J.C.J.K.) is cofounder and shareholder of OPNT bv. The authors declare no further competing interests. **Data and materials availability:** Computer code and experimental data used to obtain the results of the main text and supplementary materials are available from DataverseNL (https://hdl.handle.net/10411/QCCLF3).

SUPPLEMENTARY MATERIALS

science.sciencemag.org/content/369/6508/1238/suppl/DC1
Materials and Methods
Figs. S1 to S3
Tables S1 to S3
References (*30*–*48*)

5 November 2019; accepted 17 July 2020
Published online 30 July 2020
10.1126/science.aba0453

Proton-electron mass ratio from laser spectroscopy of HD^+ at the part-per-trillion level

Sayan Patra, M. Germann, J.-Ph. Karr, M. Haidar, L. Hilico, V. I. Korobov, F. M. J. Cozijn, K. S. E. Eikema, W. Ubachs and J. C. J. Koelemeij

Science **369** (6508), 1238-1241.
DOI: 10.1126/science.aba0453originally published online July 30, 2020

A very precise ratio

The value of the ratio of the masses of the proton and the electron has a bearing on the values of other physical constants. This ratio is known to a very high precision. Patra *et al.* improved this precision even further by measuring particular frequencies in the rovibrational spectrum of the hydrogen deuteride molecular ion (HD^+) (see the Perspective by Hori). To reach this high precision, the researchers placed the HD^+ molecules in an ion trap and surrounded them by beryllium ions. The cold beryllium ions then helped cool the HD^+ molecules, making the HD^+ spectral lines narrow enough that the proton-electron mass ratio could be extracted by comparison with theoretical predictions.

Science, this issue p. 1238; see also p. 1160